Vol. 568: 31–45, 2017
https://doi.org/10.3354/meps12045

MARINE ECOLOGY PROGRESS SERIES
Mar Ecol Prog Ser

Published March 24

Spatial and temporal variability within marine isoscapes: implications for interpreting stable isotope data from marine systems

Carolyn M. Kurle[1,*], Jennifer K. McWhorter[2,3]

[1]Division of Biological Sciences, Ecology, Behavior, and Evolution Section, University of California, San Diego, La Jolla, CA 92093, USA

[2]Scripps Institution of Oceanography, University of California, San Diego, La Jolla, CA 92093, USA

[3]*Present address:* Southern California Coastal Ocean Observing System (SCCOOS), Scripps Institution of Oceanography, University of California, San Diego, La Jolla, CA 92093, USA

ABSTRACT: Analyses of intrinsic biogeochemical markers, such as stable carbon (δ^{13}C) and nitrogen (δ^{15}N) isotopes, in animal tissues are used to investigate multiple ecological parameters for marine species. Their successful application relies on a mechanistic understanding of isotopic variations at the base of the food web because those variations influence isotope values in higher trophic level species. To better determine the potential for and mechanisms driving spatial and temporal changes in isotope values from an oceanographically complex nearshore marine system, we (1) constructed fine-scale δ^{13}C and δ^{15}N isoscapes of the Southern California Bight (SCB) using isotope values from particulate organic matter (POM) collected over 5 seasons from ~30 stations and (2) related the isotope data to geographic, seasonal, and oceanographic parameters collected from the same stations via a multimodel procedure and regression analyses. Important variables for predicting the δ^{13}C and δ^{15}N values from the POM included chlorophyll *a*, latitude, and season, and longitude, season, nitrate, and oxygen, respectively. We related these variables to seasonal shifts in nutrients most pronounced around localized eddies that concentrate upwelling. The potential for such variability should be considered when interpreting small-scale geographic and/or seasonal patterns in isotope data from species in the SCB and other dynamic coastal waters. However, the overall isotopic variability for the SCB was relatively low, with mean (±SD) δ^{13}C and δ^{15}N values of −22.7 ± 2.0‰ and 8.0 ± 1.5‰, respectively, allowing for isotopic categorization of the SCB and comparison with other Eastern Pacific coastal areas to better understand larger-scale animal migration patterns, foraging ecology, and habitat use.

KEY WORDS: δ^{13}C · δ^{15}N · Stable isotope analysis · Ecogeochemistry · Foraging ecology · Southern California Bight · California Current · Pacific Ocean

INTRODUCTION

Ecogeochemistry is the ecological application of geochemical tools to better understand community ecology questions related to animal habitat use, foraging niches, and migration patterns (McMahon et al. 2013). Practitioners of ecogeochemistry utilize intrinsic stable isotope markers in organic tissues that reflect the isotope composition at the base of the food web of interest. The stable isotope values from organismal tissues provide a direct link to species' geographic location, allowing for the reconstruction of animal foraging ecology and movement patterns (Kurle & Gudmundson 2007, Hobson et al. 2010, Ramos & Gonzalez-Solis 2012, Trueman et al. 2012). This is especially useful in ocean systems as marine vertebrates are cryptic, it is expensive and difficult to catch and track animals with geolocation tags, and

*Corresponding author: ckurle@ucsd.edu

their foraging habits frequently take place out of sight and underwater. In addition, many marine species are threatened, endangered, in conflict with anthropogenic influences, or otherwise of conservation interest, increasing the importance of understanding their ecology for the best application of conservation and management.

A common use of ecogeochemistry in marine systems is the interpretation of animal habitat use and foraging through the measurement of bulk stable carbon ($\delta^{13}C$) and nitrogen ($\delta^{15}N$) isotope values from vertebrate tissues (e.g. Kurle & Worthy 2001, 2002, Kurle & Gudmundson 2007, Newsome et al. 2010, Turner Tomaszewicz et al. 2017). However, the best application of this technique requires an understanding of the isotopic patterns from prey items or other material from the base of the food web that drive the isotope values at other trophic levels (Graham et al. 2010, Hobson et al. 2010, Jaeger et al. 2010, McMahon et al. 2013, Turner Tomaszewicz et al. 2017). Without these data, it is difficult to interpret foraging ecology patterns using bulk stable isotope values from predators because they can vary based on processes that drive the isotope values in primary production at the base of the food web (Jennings & Warr 2003, Barnes et al. 2009, Lorrain et al. 2014). For example, Kurle et al. (2011) found temporal, geographic, and ontogenetic differences in the $\delta^{13}C$ and $\delta^{15}N$ values from common marine mammal prey species collected in Alaskan waters. These differences can lead to variations in the isotope values of predators over different seasons, years, and locations, thereby confusing the foraging ecology and habitat use interpretations of the bulk stable isotope data from marine predators.

One method employed to avoid these misinterpretations is the use of compound specific stable isotope analysis of amino acids (CSIA-AA), a technique that involves analyzing the $\delta^{15}N$ values from individual amino acids from a predator's tissues (Popp et al. 2007, Chikaraishi et al. 2009, Lorrain et al. 2014). Certain 'source' amino acids show little isotopic fractionation as they are transferred up successively higher trophic levels, thereby reflecting the nitrogen isotope composition at the base of the food web (Popp et al. 2007, Chikaraishi et al. 2009). While this method is useful, it is also very time-intensive and expensive. Another technique for the better ecological interpretation of bulk stable isotope data from consumers is the construction of stable isotope maps or isoscapes that reflect the $\delta^{13}C$ and $\delta^{15}N$ values from the base of the food web (Bowen 2010).

Large-scale terrestrial isoscapes have been used successfully to track the habitat use, migration patterns, and trophic status of multiple species (Bowen 2010). Less common has been the creation and utilization of marine isoscapes. Those who have created marine isoscapes frequently use isotope values from consumers that integrate baseline stable isotope values over time to help alleviate the potential for complications involved with measuring plankton at the base of the food web, as phytoplankton blooms are ephemeral and the rate of plankton turnover is high (Schell et al. 1998, Jaeger et al. 2010, Radabaugh et al. 2013, MacKenzie et al. 2014, Vokhshoori et al. 2014, Pethybridge et al. 2015). Recent, broad-scale marine isoscapes of the Atlantic Ocean have been created utilizing meta-analyses of stable isotope data from zooplankton collected over nearly 50 yr and from multiple studies (Graham et al. 2010, McMahon et al. 2013). While these large-scale isoscapes provide a significant overview of long-term geographic variability in stable isotope values across large areas of ocean, they are missing the opportunity for more fine-scale measures of temporal and spatial variation that could lead to a better understanding of the potential for isotopic fluctuation in marine isoscapes. Because many factors drive the $\delta^{13}C$ (Rau et al. 1982, 1990, 1992, 2001, Goericke & Fry 1994, Barnes et al. 2009) and $\delta^{15}N$ (Jennings & Warr 2003, Somes et al. 2010) values at the base of marine food webs, the potential for fine-scale, biologically relevant, seasonal, annual, and geographic variability is high (Quillfeldt et al. 2015) and can be evaluated by measuring variation in stable isotope values in high-turnover, temporally dynamic primary producers such as phytoplankton.

The ratios of heavy to light isotopes for elements that circulate as part of biogeochemical cycles reflect the natural processes driving these cycles. As such, stable isotope values from various locations are different depending upon the locations' dominant processes (Gruber & Sarmiento 1997, Hobson 1999, Hobson et al. 2010, Newsome et al. 2010, Ruiz-Cooley & Gerrodette 2012). For example, in productive marine systems with low oxygen concentrations, a dominant nitrogen source to the food web is derived from denitrification, whereby microbes break down organic matter, converting organic nitrogen to inorganic nitrogen, using oxygen in the process. This process leads to an available nitrogen pool that is enriched in ^{15}N compared to areas where the nitrogen pool is dominated by nitrogen fixation (Cline & Kaplan 1975). Phytoplankton in regions dominated by denitrification take up the nitrogen with higher $\delta^{15}N$ values, and these higher values propagate up

the food web, influencing the $\delta^{15}N$ values of all consumers in that system. By measuring stable isotope values across a land- or seascape, and understanding how those values are predictably influenced by environmental and oceanographic conditions, we can create dynamic contour maps of isotopic variation that allow for a better understanding of habitat and resource utilization by organisms of interest.

The primary objectives in this study were to (1) construct fine-scale, coastal marine $\delta^{13}C$ and $\delta^{15}N$ isoscapes of the Southern California Bight (SCB) using stable isotope data from particulate organic matter (POM) collected over 5 seasons from ~30 stations for the better interpretation of marine animal habitat use and foraging ecology in the SCB, (2) determine the potential for change in the stable isotope values among seasons and between years in dynamic, nearshore systems to better understand the potential for short-term, seasonal variability in marine isoscapes, and (3) determine the oceanographic factors that drive potential isotopic differences in the SCB to better predict stable isotope values in this and other coastal marine systems.

MATERIALS AND METHODS

Study system

The SCB has been categorized as unique oceanographically for an eastern boundary current in that it serves as a transition zone between the colder, nutrient-rich, upwelled water of the California Current to the north and the warmer, subtropical, less nutrient-rich water of the Southern California Countercurrent to the south (Fig. 1) (Hickey 1979, 1993, DiGiacomo & Holt 2001, DiGiacomo et al. 2002, Gelpi & Norris 2008). Strong seasonal upwelling and variations in sea surface temperature (ranging from ~12 to ~20°C, depending on time of year and location; Gelpi & Norris 2008) and nutrient transport (e.g. nitrate flux across multiple seasons and years ranges from 4.8 ± 1.9 $kmols^{-1}$ to 14.9 ± 2.2 $kmols^{-1}$; Bograd et al. 2001), in conjunction with the convergence of these 2 major ocean currents, have the potential to drive significant temporal and spatial variations in biogeochemical responses (Hickey 1993, Jennings & Warr 2003, Barnes et al. 2009), thereby potentially increasing our understanding of the best applications of ecogeochemistry in dynamic and productive coastal systems. In addition, the oceanographic patterns within the SCB create an area of increased and variable biological productivity (Bograd et al. 2001) and diversity that contribute to its ecological importance, making it highly relevant for the application of ecogeochemical techniques (Dailey et al. 1993). For example, the SCB is a permanent or migratory home to hundreds of species including 28 pelagic seabirds, several of which are endemic, 20 species of marine mammals, including 4 species of pinnipeds that breed on the Channel Islands within the SCB, ~500 species of fish, and >5000 invertebrate species (Takekawa et al. 2004).

POM collection

In collaboration with the California Cooperative Oceanic Fisheries Investigations (CalCOFI), a long-term oceanographic monitoring program in the SCB, we collected and analyzed the $\delta^{13}C$ and $\delta^{15}N$

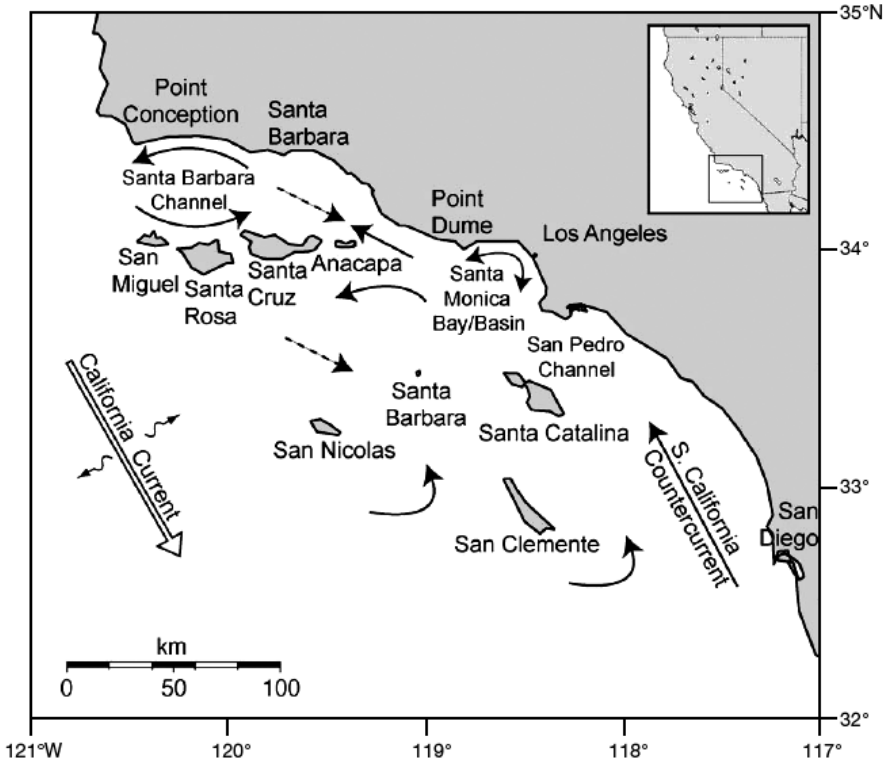

Fig. 1. Prevailing near-surface circulation in the Southern California Bight (SCB; reprinted from DiGiacomo et al. 2002 with permission). Solid arrows indicate the general SCB pattern of poleward flow nearshore and equatorward flow offshore (i.e. the California Current migrates closer to shore in spring and summer). Dashed arrows signify a shift to SCB-wide equatorward flow during spring. For a complete overview, see DiGiacomo & Holt (2001)

values from POM collected over 5 seasons in 2012 to 2013 from multiple stations in the SCB (Fig. 2, Table S1 in Supplement 2 at www.int-res.com/articles/suppl/m568p031_supp.pdf). POM was collected in summers (July 2012, 36 stations; July 2013, 30 stations), fall (October 2012, 38 stations), winter (January 2013, 35 stations), and spring (April 2013, 33 stations) (Table S1). We collected water samples at depths ranging from 8 to 12 m in either 1.04 or 2.2 l brown polypropylene bottles. Smaller volumes were collected when chlorophyll *a* (chl *a*) concentrations were higher as measured from the CTD instrument fluorometer (see next section). We filtered the POM from the water samples onto precombusted Whatman GF/F 25 mm filter papers under low vacuum pressure (40 mm Hg), folded the filter in half to protect the POM, wrapped the filter in precombusted aluminum foil, froze the entire package in liquid nitrogen on the ship, then transferred it to a –20°C freezer to await stable isotope processing in the Kurle lab at UC San Diego.

Oceanographic data collection

For each POM sample collected at each sampling date and station location (Fig. 2, Table S1), we measured sea surface temperature (SST, °C), sea surface chl *a* concentration (µg l^{-1}), nitrate (NO_3, µM), ammonia (NH_3, µM), and dissolved oxygen (O_2, ml l^{-1}) as part of the standard protocol for CalCOFI cruises. We collected all measurements at 10 m depths. We deployed a Sea-Bird Electronics CTD instrument (Seabird 911+, Serial number 3161-936) with a rosette at each station. The rosette was equipped with 24 plastic (PVC, 10 l) bottles with epoxy-coated springs and Viton O-rings. We determined oxygen, nutrient, and chl *a* measurements at sea. We collected samples for chl *a* in calibrated 138 ml polyehylene bottles and filtered them onto Whatman GF/F filters. We extracted the pigments in cold 90% acetone (Venrick & Hayward 1984) for a minimum of 24 h. We determined chl *a* concentrations from fluorescence readings before and after acidification with a Turner Designs Fluorometer Model 10-AU-005-CE. We analyzed nutrient samples at sea using an AuAAtro continuous flow analyzer (SEAL Analytical). We analyzed dissolved NO_3 using a modification of the method described by Armstrong et al. (1967) and Gordon et al. (1992), and we measured ammonia fluorometrically using a modification of the method described by Kérouel & Aminot (1997). We analyzed dissolved oxygen with an automated oxygen titrator designed by the Ocean Data Facility of Scripps Institution of Oceanography using photometric endpoint detection based on the absorption of 365 nm wavelength ultra-violet light. A computer controlled the titration of the samples and data logging. For more details on all oceanographic sampling methodology, see www.calcofi.org.

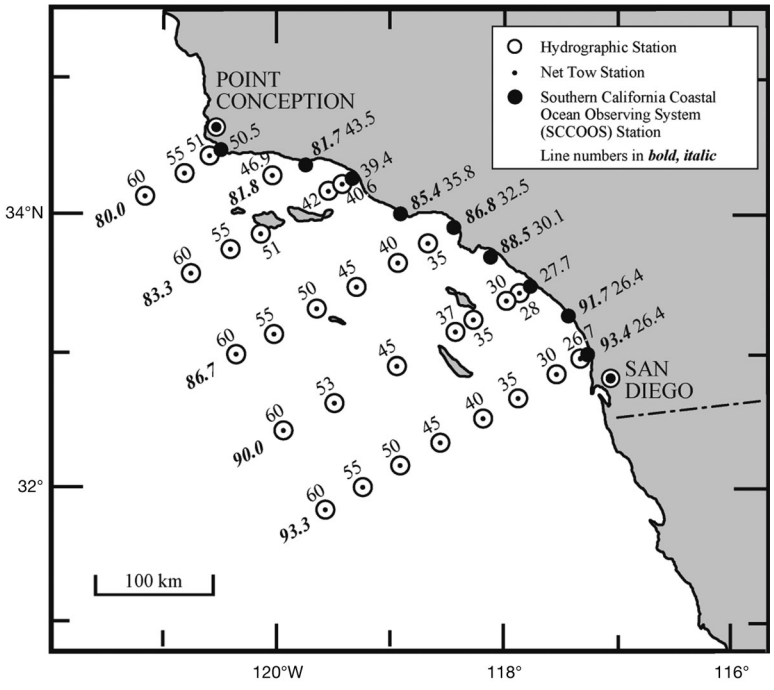

Fig. 2. The Southern California Bight and the California Cooperative Oceanic Fisheries Investigations (CalCOFI) sampling line (***bold, italic***) and station numbers where all particulate organic matter (POM) samples and oceanographic variables were collected for use in this study

Stable isotope analysis

We examined the filter paper under a dissecting scope in the lab to remove all zooplankton or other non-relevant debris, then scraped the POM from each filter paper with clean forceps, transferred the material to a cryovial, freeze-dried it for 24 h, and homogenized it by hand. We weighed ~10 to 20 mg of each sample into 5 × 9 tin capsules and sent them to the Stable Isotope Laboratory at the Department of Earth and Marine Sciences at the University of California, Santa Cruz. The $\delta^{13}C$ and $\delta^{15}N$ values were analyzed using a CE1108 elemental analyzer (Carlo Erba) interfaced via a

CONFLO III device to a Thermo-Electron Delta Plus XP mass spectrometer (Thermo-Finnigan). We calculated δ values, where

$$\delta = \left(R_{\text{sample}} / R_{\text{standard}} - 1\right) \times 1000 \quad (1)$$

and R is $^{13}C/^{12}C$ or $^{15}N/^{14}N$. The units are parts per thousand (‰) deviations from the standard. We calculated the average precision for these data as the SD of the $\delta^{13}C$ and $\delta^{15}N$ values from a set of standards (acetanilide from A. Schimmelmann, Indiana University, see Schimmelmann et al. 2009), and precision was 0.2‰ for nitrogen and 0.1‰ for carbon.

Statistical analyses

To test for the effects of geographic (latitude and longitude), temporal (season, which was treated as a continuous variable), and oceanographic (chl *a*, SST, NO_3, NH_3, and O_2) variables on the $\delta^{13}C$ and $\delta^{15}N$ values from POM collected at each station, we followed an information theoretic approach. We applied a multimodel procedure and model averaging (see Grueber et al. 2011) where we assessed the relative importance of each variable to the prediction of the $\delta^{13}C$ and $\delta^{15}N$ values by first generating global model sets with all variables, then conducting an all subsets approach wherein all combinations of all variables were compared and the top 5 models with the most important predictors were included. We generated global model sets (with all parameters described above) using the lm function in the *lme4* package in R (Bates et al. 2015), and these sets were defined as:

Model 1: lm(δ^{13}C POM ~ Season + Latitude + Longitude + SST + chl *a* + NO_3 + NH_3 + O_2, data=na.omit)

Model 2: lm(δ^{15}N POM ~ Season + Latitude + Longitude + SST + chl *a* + NO_3 + NH_3 + O_2, data=na.omit)

Then, using these model sets, we obtained the top 5 AICc of models using the dredge function in the *MuMIn* package in R (Barto 2015). *MuMIn* is a multimodel inference package and dredge conducts automatic model selection using subsets of the variables from the global models. The sets of models were generated with all possible combinations using the following function:

```
allModel1 ← dredge(model1, trace = FALSE, rank = "AICc")
(attr(allModel1, "rank.call"))
fmList2 ← get.models(allModel1, 1:5)
summary(model.avg(fmList))
```

We used Model 1 for analysis of the $\delta^{13}C$ data and Model 2 for the $\delta^{15}N$ data. We then fit regression models between the $\delta^{13}C$ or $\delta^{15}N$ values of the POM and each of the geographic, temporal, and oceanographic variables that were determined significant by our multimodel procedures to better understand the potentially predictive relationships between them. To better understand potential patterns of seasonality, we also compared the stable isotope values from the POM collected in each season using ANOVA and Tukey's honestly significant difference tests. Significance was determined at the $p = 0.05$ level.

Spatial analysis techniques

We created maps of the stable isotope data for each season in Esri's ArcGIS software (see Table S1 in Supplement 2 for the raw data, see Supplement 1 for all processing steps involved in creating the maps, and Figs. S1A–E & S2A–E in Supplement 2; all at www.int-res.com/articles/suppl/m568p031_supp.pdf). We used the inverse distance weighted interpolation method which estimates cell values by averaging each cell's value of sample data points in the 'neighborhood' or surrounding area. If a point was closer to the center of the cell being estimated, it had more influence, or weight, on the averaging process. The inverse distance weight tool has the least amount of assumptions when interpolating data. However, the data were not spatially autocorrelated, meaning not enough values were available to interpolate with certainty. Therefore, caution should be used when interpreting these isotope patterns, and the maps created from these analyses are for visual purposes and should not be taken as fact in the areas of interpolation. The graphical presentation of data with explicit or implicit disregard for their lack of spatial autocorrelation is prevalent in the marine isoscape literature, and we recognize our data are similarly problematic. However, multiple publications still present these representations (e.g. Schell et al. 1998, McMahon et al. 2013, Radabaugh et al. 2013, Quillfeldt et al. 2015) as they are useful for visualizing data, so we have included similar maps in Supplement 2 (Figs. S1A–E & S2A–E). In addition, because our data lacked spatial autocorrelation, we focused instead on examining the standard deviations around the mean $\delta^{13}C$ and $\delta^{15}N$ values for each geographic point over the 5 seasons of data collection and relating those variations to specific oceanographic and environmental variables to better understand the potential drivers of seasonal isotopic variation.

RESULTS

Geographic, temporal, and oceanographic variables and the $\delta^{13}C$ and $\delta^{15}N$ values from POM

The $\delta^{13}C$ values measured within the SCB across seasons and locations ranged from −27.2 to −13.5‰ with a mean of −22.7 ± SD 2.0‰. Using the multimodel procedure and model averaging described above, we found that 5 variables were consistently important for predicting the $\delta^{13}C$ values from the POM and were included in all top 5 models: chl *a* ($p < 0.01$), latitude ($p = 0.04$), longitude ($p = 0.03$), season ($p < 0.01$ for all seasons with fall 2012 as the reference category), and SST ($p = 0.01$). The model with the lowest AICc value (619.24) also included NO_3; however, its effect was not significant ($p = 0.39$), and it was only included in 3 of the 5 best models, so it was not considered a significant predictor (Table 1). The AICc values for the top 5 models ranged from 619.24 to 621.13. To better understand the relationships between these variables and the $\delta^{13}C$ values from the POM, we fit them to regression models. There were clear linear relationships between the POM $\delta^{13}C$ values and chl *a* (adj. $R^2 = 0.13$, $F = 27.2$, $p > 0.01$), latitude (adj. $R^2 = 0.12$, $F = 24.3$, $p < 0.01$), and season (adj. $R^2 = 0.25$, $F = 57.2$, $p < 0.01$) (Fig. 3A–C); however, neither SST (adj. $R^2 = -0.001$, $F = 0.84$, $p = 0.36$) nor longitude (adj. $R^2 = -0.001$, $F = 0.76$, $p = 0.38$) were significantly correlated with POM $\delta^{13}C$ values. To further understand relationships between seasons and the $\delta^{13}C$ values from the POM, we compared those values among seasons, and there were significant differences (ANOVA, $F_{4,167} = 18.9$, $p < 0.01$). The POM collected in summer 2012 had significantly higher $\delta^{13}C$ values than fall 2012 and winter, spring, and summer 2013 (Tukey's, all $p < 0.01$) and fall 2012 had higher $\delta^{13}C$ values than summer 2013 (Tukey's, $p = 0.02$), but the $\delta^{13}C$ values from the POM collected in all other seasons were not significantly different (Tukey's, $0.15 \leq p \leq 1.0$) (Fig. 3C).

The $\delta^{15}N$ values measured within the SCB across seasons and locations ranged from 3.5 to 11.9‰ with a mean (± SD) of 8.0 ± 1.5‰. Using the multimodel procedure and model averaging described above in 'Statistical analyses', 4 variables were consistently important in all top 5 models for predicting the $\delta^{15}N$ values from POM: longitude ($p < 0.01$), NO_3 ($p < 0.01$), O_2 ($p < 0.01$), and season. However, with fall 2012 as the reference category for the season parameter, only spring and summer 2013 were significant predictors ($p \leq 0.01$), whereas summer 2012 ($p = 0.73$) and winter 2013 ($p = 0.92$) were not (Table 1). The AICc values for the top 5 models ranged from 549.16 to 551.97. We fit these 4 variables and the $\delta^{15}N$ values from the POM to linear regression models, and all but O_2 were significantly related (Fig. 4A–C) (longitude: adj. $R^2 = 0.17$, $F = 34.87$, $p < 0.01$; season: adj. $R^2 = 0.06$, $F = 11.47$, $p < 0.01$; NO_3: adj. $R^2 = 0.09$, $F = 18.16$, $p < 0.01$; O_2: adj. $R^2 = -0.01$, $F = 0.13$, $p = 0.72$). The top model with the lowest AICc value (549.16) included 6 variables (the 4 listed plus SST and NH_3), but SST and NH_3 were not significant predictors based on this analysis ($p = 0.11$ and $p = 0.10$, respec-

Table 1. Summary results after model averaging: effects of each parameter on the $\delta^{13}C$ or $\delta^{15}N$ values (‰) from particulate organic matter (POM) collected at California Cooperative Oceanic Fisheries Investigations (CalCOFI) stations throughout the Southern California Bight (see text, Fig. 1 and Table S1 [in Supplement 2 at www.int-res.com/articles/suppl/568p031supp.pdf] for details on isotope values, stations, locations, timing, and oceanographic variables). A relative importance score of 1 indicates inclusion of that parameter in all 5 of the models

Parameter	Estimate	Adjusted SE	p-value	Relative importance
$\delta^{13}C$				
(Intercept)	1.631	16.951	0.92	–
Chl *a* (μg l^{-1})	0.287	0.074	<<0.01	1.00
Latitude	0.420	0.200	0.04	1.00
Longitude	−0.269	0.127	0.03	1.00
NO_3 (μM)	−0.095	0.061	0.12	0.60
Season (Spring 2013)[a]	−2.541	0.559	<<0.01	1.00
Season (Summer 2012)	0.988	0.369	0.01	1.00
Season (Summer 2013)	−2.003	0.396	<<0.01	1.00
Season (Winter 2013)	−2.456	0.577	<<0.01	1.00
SST (°C)	−0.341	0.123	0.01	1.00
NH_3 (μM)	0.331	0.309	0.29	0.33
O_2 (ml l^{-1})	−0.231	0.371	0.53	0.12
$\delta^{15}N$				
(Intercept)	74.676	14.267	<<0.01	–
Longitude	−0.499	0.108	<<0.01	1.00
NH_3 (μM)	−0.536	0.290	0.03	0.89
NO_3 (μM)	−0.280	0.062	<<0.01	1.00
O_2 (ml l^{-1})	−0.864	0.299	<0.01	1.00
Season (Spring 2013)[a]	1.118	0.459	0.01	1.00
Season (Summer 2012)	0.115	0.338	0.73	1.00
Season (Summer 2013)	1.247	0.325	<<0.01	1.00
Season (Winter 2013)	0.048	0.484	0.92	1.00
SST (°C)	−0.197	0.096	0.04	0.89
Latitude	0.122	0.157	0.44	0.19
Chl *a* (μg l^{-1})	−0.019	0.057	0.73	0.15

[a]Fall 2012 was the reference category for the season parameter

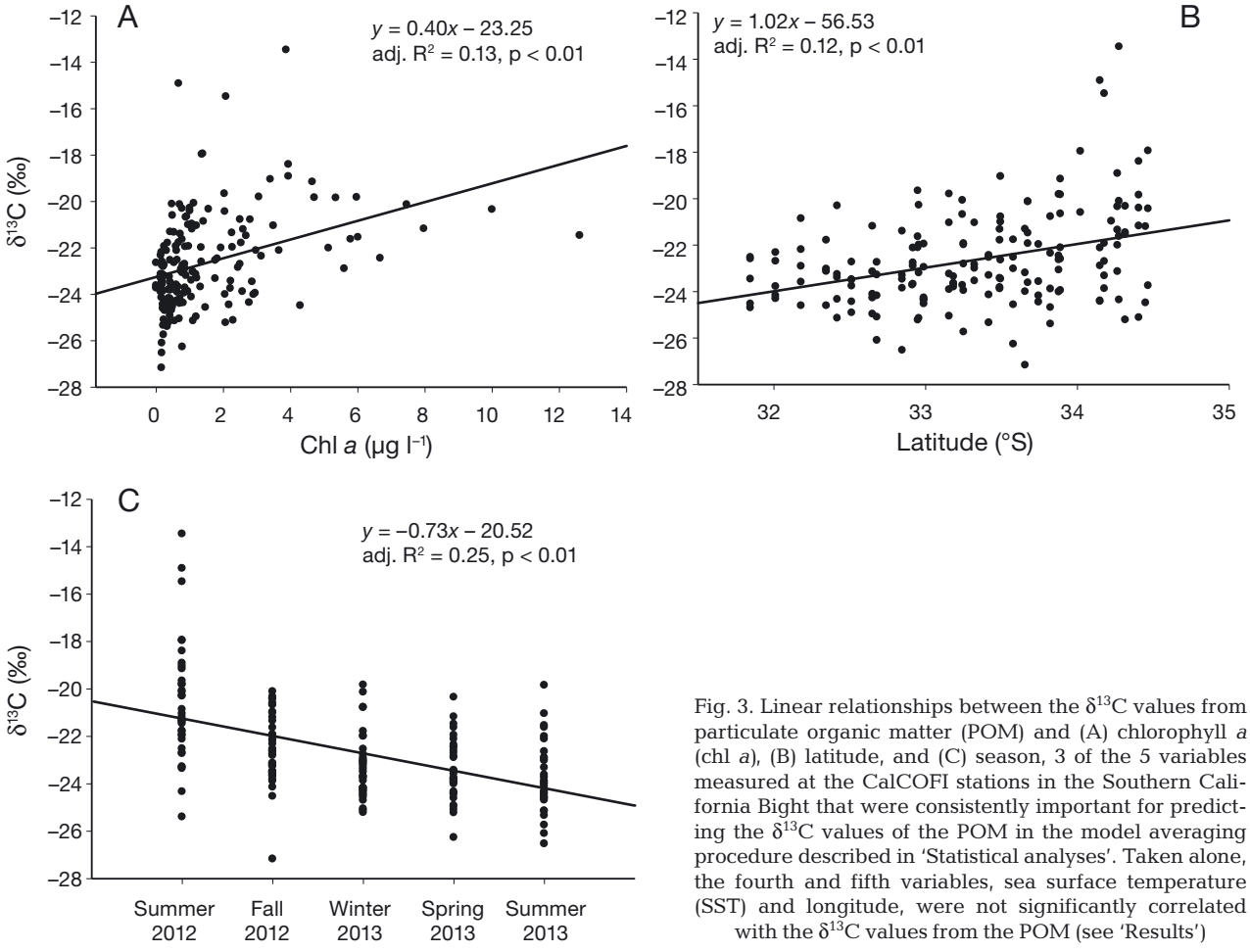

Fig. 3. Linear relationships between the $\delta^{13}C$ values from particulate organic matter (POM) and (A) chlorophyll *a* (chl *a*), (B) latitude, and (C) season, 3 of the 5 variables measured at the CalCOFI stations in the Southern California Bight that were consistently important for predicting the $\delta^{13}C$ values of the POM in the model averaging procedure described in 'Statistical analyses'. Taken alone, the fourth and fifth variables, sea surface temperature (SST) and longitude, were not significantly correlated with the $\delta^{13}C$ values from the POM (see 'Results')

tively). However, SST alone was significantly related to the POM $\delta^{15}N$ values, and a 3 parameter Gaussian nonlinear regression model ($f(x) = 8.6e^{(-0.5)\left(\frac{x-16.5}{6.9}\right)^2}$; $F = 13.1$, $p < 0.01$) fit the data well (Fig. 4D), indicating that the $\delta^{15}N$ values from POM increased with increasing temperature up to a midway point of ~16°C whereupon the $\delta^{15}N$ values decreased with increasing temperature up to the maximum of ~20°C. To further understand relationships between seasons and the $\delta^{15}N$ values from the POM, we compared values among seasons: there were significant differences (ANOVA, $F_{4,167} = 3.4$, $p = 0.01$), but only summer 2013 had significantly higher $\delta^{15}N$ values than summer and fall 2012, and winter 2013 (Tukey's, $p = 0.01$, 0.05, and 0.04, respectively). The $\delta^{15}N$ values from POM collected in spring and summer 2013 were not different from each other, nor were the values from POM different between any of the other seasons (Tukey's test, $0.44 \leq p \leq 1.0$) (Fig. 4B).

Marine isoscapes

There were clear visual differences in the $\delta^{13}C$ and $\delta^{15}N$ values from POM collected at each station among seasons and geographic areas within the SCB that were apparent in the seasonal isoscapes generated in ArcGIS (Figs. S1A–E & S2A–E) and by the maps depicting the standard deviations of the means of the $\delta^{13}C$ and $\delta^{15}N$ values from the POM collected over the 5 seasons (Fig. 5A,B). The highest seasonal variations around the mean (±SD) $\delta^{13}C$ values were observed at Stn 60 in Line 80 (±3.9‰; near Pt. Conception and the southern edge of the California Current), Stns 50.5 and 51 in Line 80.0, Stn 43.5 in Line 81.7, and Stn 46.9 in Line 81.8 (range from ± 2.3 to 4.6‰; the Santa Barbara Channel), Stn 42 in Line 83.3 (±3.4‰; south of the Santa Barbara Channel), and Stn 40 in Line 86.7 (±2.4‰; the Santa Monica/San Pedro Basin Eddy) (Figs. 2 & 5A), and the highest seasonal variation around the mean $\delta^{15}N$ values (±2.7‰) was observed at Stn 46.9 in Line 81.8 (the Santa Barbara Channel) (Figs. 2 & 5B).

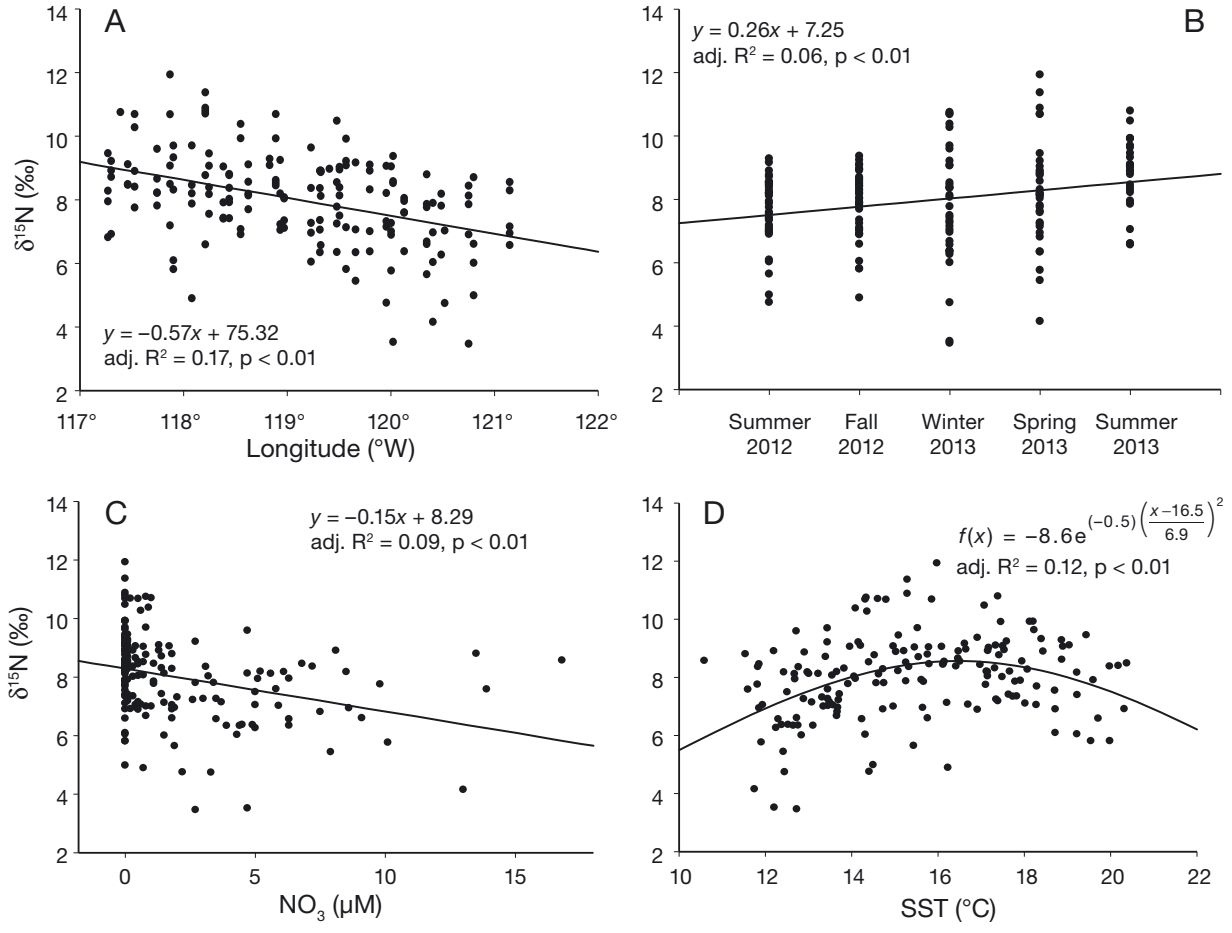

Fig. 4. Linear relationships between the $\delta^{15}N$ values from particulate organic matter (POM) and (A) longitude, (B) season, and (C) nitrate (NO_3), 3 of the 4 variables measured at the CalCOFI stations in the Southern California Bight that were consistently important for predicting the $\delta^{15}N$ values of the POM in the model averaging procedure described in 'Statistical analyses'. Taken alone, the fourth variable, O_2, was not significantly correlated with the $\delta^{15}N$ values from the POM (see 'Results'). Sea surface temperature (SST), while not a significant variable in the multimodel averaging analysis, was significantly related to the POM $\delta^{15}N$ values when taken alone as demonstrated by (D) a 3 parameter Gaussian nonlinear regression model

DISCUSSION

The results of our model averaging procedures and various models indicate that several variables are important for predicting spatial and temporal variation in the $\delta^{13}C$ and $\delta^{15}N$ values from POM across the SCB. However, many of these variables are likely driven by seasonally and spatially variable patterns in upwelling that influence nutrient availability and primary production and therefore affect the stable isotope values of the POM. We do not have upwelling data for each of the stations at which we measured stable isotope values. We do, however, have the upwelling indices measured from within the SCB for the time of our study, and we measured several parameters that relate directly to upwelling patterns that can be used to infer causal relationships between upwelled nutrients and stable isotope values in the SCB.

Based on the multimodel procedure, model averaging, and regression models, longitude, season, NO_3, and SST appear to be the most important influences on the $\delta^{15}N$ values of the POM. As stated above, the model averaging analysis allows for the simultaneous examination of multiple models, which is valuable because certain variables may only be important when taken in context with other variables. For instance, in our study (Fig. 6A) and in the SCB in general, SST strongly follows the season (highest in summer/fall, lowest in winter/spring; Gelpi & Norris 2008), seasonally variable upwelling and winter convection are the strongest drivers of nutrient availability and primary productivity cycles in the SCB (Mantyla et al. 2008, Bograd et al. 2009), and infusion

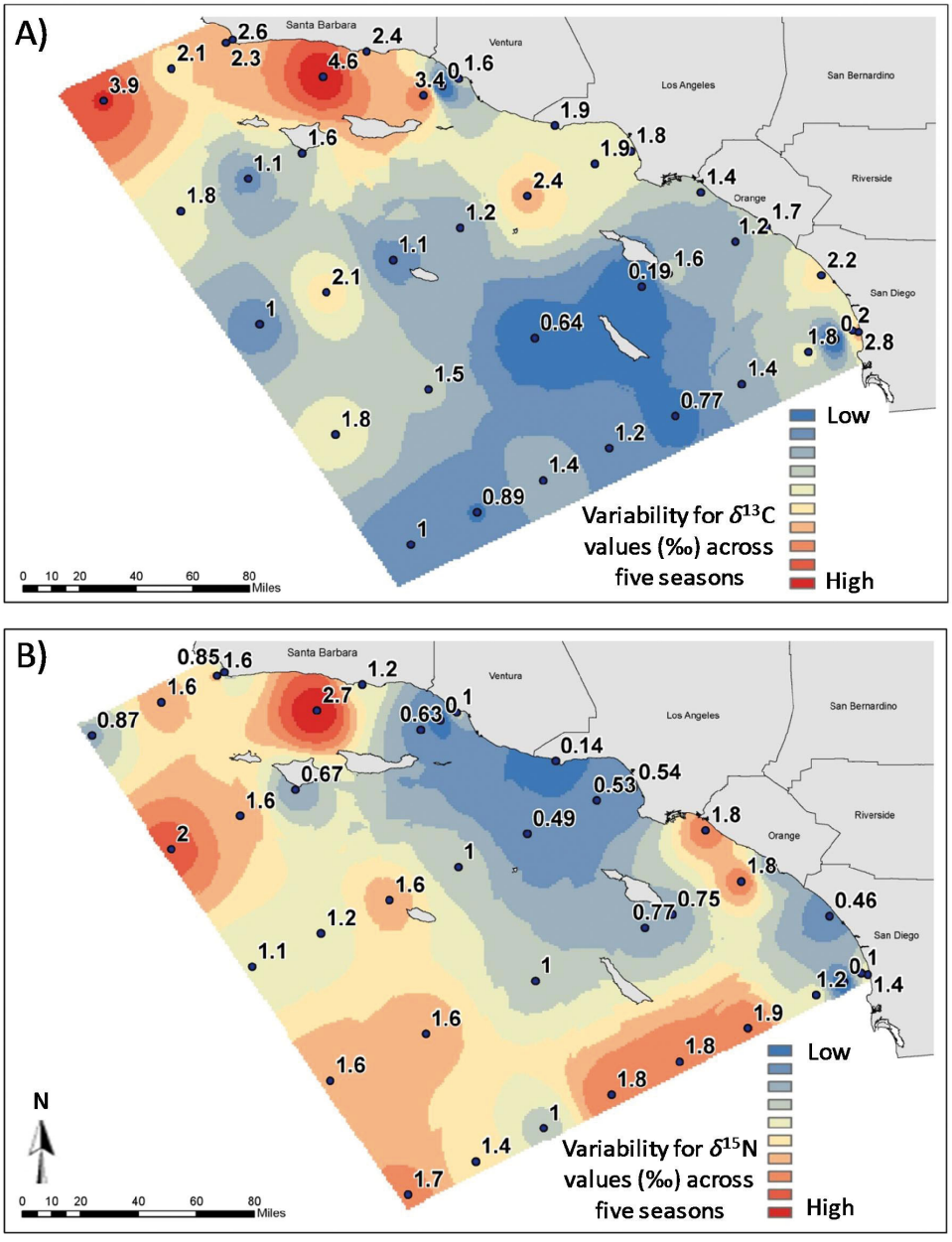

Fig. 5. Standard deviations (SD) around the mean (A) $\delta^{13}C$ and (B) $\delta^{15}N$ values (‰) from particulate organic matter (POM) collected at CalCOFI stations over 5 seasons (summer 2012, fall 2012, winter 2013, spring 2013, and summer 2013). Interpolation (color) was added for visualization purposes (see 'Materials and methods'). For isoscape maps of the $\delta^{13}C$ and $\delta^{15}N$ values for each season, see Figs. S1A–E & S2A–E, respectively, in Supplement 2 at www.int-res.com/articles/suppl/m568p031_supp.pdf

of NO_3 into marine systems from seasonal upwelling is a strong driver of POM $\delta^{15}N$ values (Nakatsuka et al. 1992, Altabet 2001). Therefore, SST, season, and NO_3 would be strongly correlated with one another and with the temporal variability observed in the measured $\delta^{15}N$ values from POM in the SCB. Indeed, the relationship between SST and NO_3 (Fig. 6B) indicates a curvilinear model fit (polynomial, inverse third order):

$$f = y_0 + \left(\frac{a}{x}\right) + \left(\frac{b}{x^2}\right) + \left(\frac{c}{x^3}\right)$$

or

$$f = -37.3 + \left(\frac{2124.4}{x}\right) + \left(\frac{-40344.9}{x^2}\right) + \left(\frac{256055.4}{x^3}\right) ;$$

adj. $R^2 = 0.80$, $F = 223.64$, $p < 0.0001$), wherein NO_3 concentration is highest at the lowest SST values.

During our study period, the mean (±SD) SSTs in winter (13.3 ± 0.9°C) and spring (13.4 ± 1.4°C)

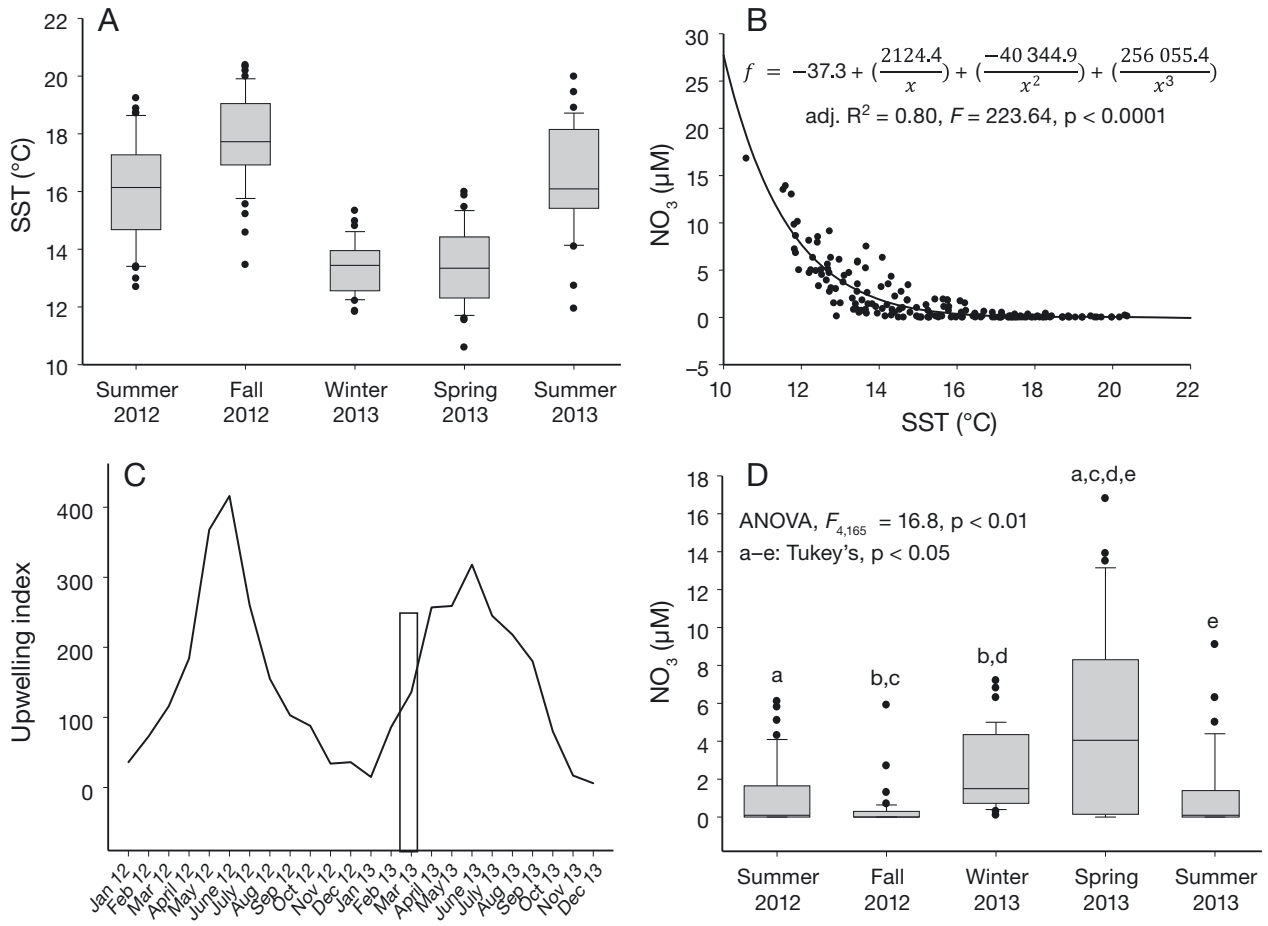

Fig. 6. Relationships between sea surface temperature (SST) and (A) season and (B) nitrate (NO_3) concentration as measured at the CalCOFI stations in the Southern California Bight (SCB). (C) The upwelling index, as measured by the metric tons of water per second per 100 m of coast, in the SCB, varied predictably with season, and the maximum upwelling that occurred during our study period (as indicated by the box) coincides with the lowest temperatures (March/spring 2013) and (D) the maximum NO_3 concentrations (spring 2013). Boxplots (A) and (D) indicate median, upper and lower 75th and 25th percentiles; whiskers represent 10th and 90th percentiles, and dots represent values outside the 10th and 90th percentiles

2013 were significantly lower than those in the other 3 seasons (16.0 ± 1.8 to 17.8 ± 1.6°C) (Fig. 6A; ANOVA, $F_{4,167}$ = 18.9, p < 0.01; Tukey's p < 0.01), which corresponded to the time of maximum upwelling in 2013 (~March 13; Fig. 6C, monthly mean upwelling index values collected in the SCB at 33° N, 119° W, available at www.pfeg.noaa.gov/products/PFEL/modeled/indices/upwelling/NA/data_download.html). NO_3 concentrations increase with increasing seasonal upwelling in the SCB, and NO_3 concentrations in the water reached their maximum in spring 2013 (Fig. 6D). The δ^{15}N values from POM were negatively correlated with the NO_3 concentrations in the water (Fig. 4C) because, as NO_3 is taken up by phytoplankton, the nutrients in the water become depleted and NO_3 concentration decreases. As the phytoplankton take up the nitrate, the nitrogen fractionates, increasing the δ^{15}N values in the phytoplankton or POM (Nakatsuka et al. 1992, Altabet 2001). Thus, the δ^{15}N values from POM are lowest at the highest levels of seasonal upwelling (late winter/early spring), which corresponds to the highest levels of NO_3 and the lowest SSTs. Season, NO_3 concentrations, and SST are therefore all related to the fluctuations in the upwelling indices and are potentially useful predictors of variability in the δ^{15}N values of POM in the SCB.

Seasonal patterns in upwelling likely influence the δ^{13}C values from POM as well. As outlined above, nutrient availability is driven by upwelling in the SCB which in turn drives productivity which contributes strongly to the δ^{13}C values from POM. Season, latitude, longitude, chl *a*, and SST were indicated by the multimodel procedure and model averaging to be

the most important drivers of the $\delta^{13}C$ values of the POM. As with the $\delta^{15}N$ values, this analysis allowed us to investigate variables that may only be important for influencing the $\delta^{13}C$ values when taken in context with other variables. For instance, when taken alone, neither SST nor longitude were significantly related to the $\delta^{13}C$ values from the POM (linear regressions, adj. $R^2 = -0.001$ for both, $p = 0.36$ and 0.38, respectively). However, as stated above, SST is strongly correlated with season in the SCB (Gelpi & Norris 2008), and upwelling, a strong driver of nutrient availability, is also highly variable by season (Mantyla et al. 2008, Bograd et al. 2009). Infusion of nutrients into marine systems from seasonal upwelling drives productivity, which is represented by the chl *a* concentrations. In our data, chl *a* concentrations were highest at the lowest temperatures (Fig. 7; single, 2 parameter, exponential decay model, $f = a^{(-bx)}$ or $f = 48.95^{(-0.23x)}$, adj. $R^2 = 0.18$, $F = 35.8$, $p < 0.0001$), which corresponded to winter and spring 2013 (Fig. 6A); the NO_3 values referred to above were also highest during the lowest temperatures (Fig. 6B), and all of these factors coincide with the period of highest upwelling (Fig. 6C).

Productivity is positively correlated with the $\delta^{13}C$ values of POM in marine systems because higher phytoplankton growth rates that occur during times of higher nutrient input lead to higher phytoplankton $\delta^{13}C$ values (Bidigare et al. 1997, Popp et al. 1998, Schell 2000). Interestingly, one may expect to see lower $\delta^{13}C$ values during times of lower SST as lower temperatures are associated with increased solubility in CO_2 and a resultant decrease in the $\delta^{13}C$ values from POM (Rau et al. 1989, Raven et al. 1993). This has been postulated to influence a longer-term decrease in $\delta^{13}C$ values in sperm whales since 1993 in the offshore California Current System (Ruiz-Cooley et al. 2014). In addition, upwelled water in the Pacific typically contains high levels of CO_2 (Capone & Hutchins 2013), which also correlates with lower $\delta^{13}C$ values in plankton (Raven et al. 1993). However, we did not see these patterns of lower $\delta^{13}C$ values with lower SST or increasing CO_2 in our data. This follows previous research demonstrating that influxes of nutrients increase phytoplankton photosynthesis, growth rate, and yield significantly more than influxes of additional inorganic carbon (Raven et al. 1993, Raven 1994). Thus, the pattern observed in our data of increasing $\delta^{13}C$ values with increasing chl *a* (Fig. 3A) is likely driven by temporal shifts in productivity fueled by predictable, seasonally upwelled and convected nutrients (Mantyla et al. 2008). Chl *a* can also be influenced by seasonally variable grazing pressure in marine systems (Longhurst 1995). However, while data indicate that grazing pressure varies seasonally in the SCB, grazing as a measure of the percentage of chlorophyll standing stock removed per day shows no consistent seasonal trends (Landry et al. 1994).

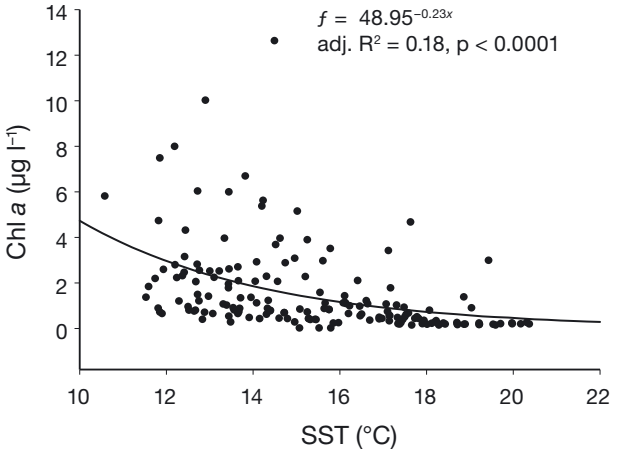

Fig. 7. Chlorophyll *a* (chl *a*) concentrations were highest at the lowest sea surface temperatures (SST) as measured at CalCOFI stations in the Southern California Bight. The lowest temperatures corresponded to winter and spring 2013

Upwelling is also likely driving the higher seasonal variance observed around the means for both the $\delta^{13}C$ and $\delta^{15}N$ values in certain regions within the SCB that are dominated by oceanographic features, such as eddies, that can lead to exaggerated levels of seasonally variable, geographically constrained, upwelled nutrients (Fig. 5A,B) (Owen 1980, Harms & Winant 1998, DiGiacomo & Holt 2001, DiGiacomo et al. 2002, Hickey et al. 2003, Mantyla et al. 2008). There are 2 areas dominated by small-scale (<50 km in diameter), coastal ocean eddies in the SCB that vary seasonally in their intensity, are important drivers of nutrients and overall productivity in the SCB, and exhibit high degrees of variation around the seasonal means for stable isotope values (DiGiacomo & Holt 2001). First, the 'hotspot' for the highest degree of variance around the means (±SD) for the $\delta^{13}C$ (±4.6‰; range: −24.4 to −13.5‰) and $\delta^{15}N$ (±2.7‰; range: 3.5 to 9.4‰) values from the POM collected across the seasons was observed in the Santa Barbara Channel at Stn 46.9 in Line 81.8 (Figs. 2 & 5A,B, see Figs. S1A–E & S2A–E). This corresponds to year-round, cyclonic eddies driven by currents extending southward from the California Current and that vary in intensity depending upon the season (Owen 1980, Harms & Winant 1998, DiGiacomo & Holt 2001). In late winter and into spring, the current is closer to shore, contributing to stronger eddies and conse-

quently more upwelled nutrients which would lead to seasonally variable stable isotope values. Second, we observed relatively high variability around the mean (±SD) δ^{13}C values at Stn 40 in line 86.7 (±2.4‰; range: −27.2 to −21.3‰) (Fig. 2) in the Santa Monica/San Pedro Basin. This area is also dominated by small-scale, recurrent eddies that exhibit seasonal variations in intensity and subsequent upwelling (Hickey 1992, DiGiacomo & Holt 2001, Hickey et al. 2003). This area has also been shown to have core temperature up to ~2°C cooler than surrounding water (DiGiacomo et al. 2016), another potential contributor to variable δ^{13}C values. Finally, we observed 2 additional areas of relatively high variability around the mean δ^{13}C values: one at Stn 60 in Line 80 near Point Conception (±SD 3.9‰; range: −22.1 to −14.9‰) (Fig. 2) and one at Stn 42 in Line 83.3 south of Point Conception (±SD 3.4‰; range: −23.9 to −15.5‰) (Fig. 2). The first is a transition zone subject to significant seasonal fluctuations in coastal upwelling that are dependent upon multiple processes, including seasonal wind patterns (Chelton 1984, Lynn & Simpson 1987, Hickey 1992, 1993, Harms & Winant 1998, Blanchette et al. 2007). The second is an area that experiences pronounced seasonal shifts in near-surface circulation (see Fig. 1 and DiGiacomo et al. 2002). It is not clear why these 3 areas do not also exhibit wider fluctuations in their seasonal δ^{15}N values that correspond with those observed in the δ^{13}C values. There are other areas within the SCB that exhibit very small-scale (1 to 20 km in diameter), seasonally variable eddies, but their prevalence and size are diminished compared to those observed in the areas of the Santa Barbara Channel and Santa Monica/San Pedro Basin (DiGiacomo & Holt 2001), and we did not see similar degrees of seasonal isotopic variability for these other areas.

Latitude and longitude are also both included in all 5 of the models that best explain the variation in POM δ^{13}C values. However, δ^{13}C values in marine systems generally decrease with increasing latitude (Rubenstein & Hobson 2004), which is opposite of what we observed with the δ^{13}C values from the POM in our study, and they are observed to increase or decrease with increasing longitude depending upon the ocean basin (e.g. Laakmann & Auel 2010, Kurle et al. 2011). The potential effects of latitude and longitude on the POM δ^{13}C values were likely confounded by the effects of distance from shore. In the SCB, latitude and longitude are related to distance from shore, with distance to shore decreasing with increasing latitude (linear regression, adj. R^2 = 0.48, F = 159.37, $p < 0.01$) and decreasing longitude (linear regression, adj. R^2 = 0.16, F = 32.11, $p < 0.01$; see Fig. 2). The δ^{13}C values in marine systems are higher in nearshore waters (Dunton et al. 1989, Hobson et al. 1994), and the increasing proximity to shore is positively related to the δ^{13}C values from the POM in our study (linear regression, adj. R^2 = 0.09, F = 17.20, $p < 0.01$). Therefore, increasing latitude and decreasing longitude are likely reflections of closer proximity to shore which are then reflected in higher δ^{13}C values from the POM.

Finally, due to the expensive nature of oceanographic cruises coupled with the limitations imposed by opportunistic sampling, we were only able to sample the POM once per station per season. Thus, we recognize that the broad generalizations regarding seasonal variations in the stable isotope values from the POM collected at each station may be a misrepresentation of the entire season as, by chance, we may have sampled, for example, during a short-lived phytoplankton bloom or after such a bloom, thereby over- or underrepresenting certain parameters in our data. However, as our stable isotope data logically follow what would be expected with increased seasonal upwelling in winter/spring and concentrated upwelling around localized eddies, we are assured the isotope data reflect reasonable seasonal expectations.

In conclusion, we observed temporal and spatial variation in the δ^{13}C and δ^{15}N values from POM collected within the SCB and largely attribute those variations to seasonal shifts in upwelled nutrients. Variability in the stable isotope values was most exaggerated in areas of localized eddies, and these seasonal and geographic differences should be considered when studying small-scale patterns of animal habitat use in this region and other highly dynamic coastal waters. The circulation patterns in the SCB are more complex and differ considerably from those elsewhere along the western coast of north America (DiGiacomo & Holt 2001, Brink & Robinson 2005). In addition, especially complicated coastal features such as multiple nearshore islands, coastal outcroppings, and submarine canyons, combined with spatially and temporally fluctuating wind and wave patterns, make the SCB flow regime especially variable (Owen 1980, Hickey 1992, 1993, DiGiacomo & Holt 2001, DiGiacomo et al. 2002). Therefore, the fluctuations in stable isotope values we observed, especially around the 2 major eddy systems, may be especially large in comparison with other, less dynamic nearshore regions, even those with considerable shifts in seasonal upwelling.

Despite the localized seasonal variability we observed in stable isotope values, the overall isotopic

variability for the SCB was relatively low. The mean $\delta^{13}C$ and $\delta^{15}N$ values were −22.7 ± 2.0‰ and 8.0 ± 1.5‰, respectively, making it possible to isotopically categorize the SCB such that it can be compared to other areas along the west coast of North America. For example, POM has $\delta^{13}C$ and $\delta^{15}N$ values from −24.1 to −19.8‰ and 6.9 to 15.1‰, respectively, from the inner shelf of the southeastern Bering Sea (Smith et al. 2002), −24.1 to −19.0‰ and 8.0 to 11.0‰, respectively, from nearshore waters off western Canada (Wu et al. 1999), and −18.9 ± 0.7‰ and 12.3 ± 1.8‰, respectively, from the Gulf of California (Altabet et al. 1999). Therefore, the SCB can be isotopically classified such that it is possible for large-scale comparisons of animal movement patterns through coastal waters of the eastern Pacific Ocean, provided they spend adequate time foraging in the SCB to incorporate its unique isotope values into their tissues (Kurle 2009). Our results underscore the need for further data collection in the building and utilization of both small- and large-scale marine isoscapes and in the understanding of how stable isotope values fluctuate with seasonal, oceanographic, and climate processes.

Acknowledgements. Thank you to the California Cooperative Oceanic Fisheries Investigations (CalCOFI) personnel, especially S. Dovel, for sample collection and assistance with data organization; to L. Aluwihare, H. Batchelor, R. Goericke, M. Ohman, and B. Semmons for project guidance; and to 2 anonymous reviewers for their valuable comments on the manuscript. Funding was provided by the MAS-MBC Capstone Program at Scripps Institution of Oceanography and the University of California San Diego.

LITERATURE CITED

Altabet M (2001) Nitrogen isotopic evidence for micronutrient control of fractional NO_3^- utilization in the equatorial Pacific. Limnol Oceanogr 46:368–380

Altabet M, Pilskaln C, Thunell R, Pride C, Sigman D, Chavez F, Francois R (1999) The nitrogen isotope biogeochemistry of sinking particles from the margin of the eastern North Pacific. Deep Sea Res I 46:655–679

Armstrong F, Stearns C, Strickland J (1967) The measurement of upwelling and subsequent biological processes by means of the Technicon Autoanalyzer and associated equipment. Deep-Sea Res 14:381–389

Barnes C, Jennings S, Barry J (2009) Environmental correlates of large-scale spatial variation in the $\delta^{13}C$ of marine animals. Estuar Coast Shelf Sci 81:368–374

Barto K (2015) MuMIn: multi-model inference. R package version 1.13.4. R Centre for Statistical Computing, Vienna

Bates D, Maechler M, Bolker B, Walker S, Christensen R, Singmann H, Dai B (2015) Linear mixed-effects models using Eigen and S4. R package version 1.1-7. R Centre for Statistical Computing, Vienna

Bidigare RR, Fluegge A, Freeman KH, Hanson KL and others (1997) Consistent fraction of ^{13}C in nature and in the laboratory: growth-rate effects in some haptophyte algae. Global Biogeochem Cycles 11:279–292

Blanchette C, Helmuth B, Gaines S (2007) Spatial patterns of growth in the mussel, *Mytilus californianus*, across a major oceanographic and biogoegraphic boundary at Point Conception, California, USA. J Exp Mar Biol Ecol 340:126–148

Bograd S, Chereskin T, Roemmich D (2001) Transport of mass, heat, salt, and nutrients in the southern California Current System: annual cycle and interannual variability. J Geophys Res 106:9255–9275

Bograd S, Schroeder I, Sarkar N, Qiu Z, Sydeman W, Schwing F (2009) Phenology of coastal upwelling in the California Current. Geophys Res Lett 36:L01602

Bowen G (2010) Isoscapes: spatial pattern in isotopic biogeochemistry. Annu Rev Earth Planet Sci 38:161–187

Brink K, Robinson A (2005) The global coastal ocean — regional studies and syntheses, Vol 11. Harvard University Press, Cambridge, MA

Capone D, Hutchins D (2013) Microbial biogeochemistry of coastal upwelling regimes in a changing ocean. Nat Geosci 6:711–717

Chelton D (1984) Seasonal variability of alongshore geostrophic velocity off central California. J Geophys Res 89: 3473–3486

Chikaraishi Y, Ogawa N, Kashiyama Y, Takano Y and others (2009) Determination of aquatic food-web structure based on compound-specific nitrogen isotopic composition of amino acids. Limnol Oceanogr Methods 7: 740–750

Cline J, Kaplan I (1975) Isotopic fractionation of dissolved nitrate during denitrification in the eastern tropical North Pacific Ocean. Mar Chem 3:271–279

Dailey M, Anderson J, Reish D, Gorsline D (1993) The Southern California Bight: background and setting. In: Dailey M, Reish D, Anderson J (eds) Ecology of the Southern California Bight. University of California Press, Berkeley, CA, p 1–18

DiGiacomo P, Holt B (2001) Satellite observations of small coastal ocean eddies in the Southern California Bight. J Geophys Res 106:22521–22543

DiGiacomo P, Hamner W, Hamner P, Caldeira R (2002) Phalaropes feeding at a coastal front in Santa Monica Bay, California. J Mar Syst 37:199–212

DiGiacomo P, Holt B, Perry B (2016) Oceanography of the Southern California Bight. https://web.csulb.edu/depts/geology/facultypages/bperry/Southern%20California%20Bight/homepage.htm (assessed December 7, 2016)

Dunton KH, Saupe SM, Golikov LN, Schell DM, Schonberg SV (1989) Trophic relationships and isotopic gradients among arctic and subarctic marine fauna. Mar Ecol Prog Ser 56:89–97

Gelpi C, Norris K (2008) Seasonal temperature dynamics of the upper ocean in the Southern California Bight. J Geophys Res 113:C04034

Goericke R, Fry B (1994) Variations in marine plankton $\delta^{13}C$ with latitude, temperature, and dissolved CO_2 in the world ocean. Global Biogeochem Cycles 8:85–90

Gordon L, Jennings J, Ross A, Krest J (1992) A suggested protocol for continuous flow automated analysis of seawater nutrients in the WOCE Hydrographic Program and the Joint Global Ocean Fluxes Study. Group Tech Rep 92-1. Oregon State University, Corvallis, OR

Graham B, Koch P, Newsome S, McMahon K, Aurioles D (2010) Using isoscapes to trace movements and foraging behavior of top predators in oceanic ecosystems. In: West J, Bowen G, Dawson T, Tu K (eds) Isoscapes: understanding movement, pattern, and process on Earth through isotope mapping. Springer, Berlin, p 299–334

Gruber N, Sarmiento J (1997) Global patterns of marine nitrogen fixation and denitrification. Global Biogeochem Cycles 11:235–266

Grueber C, Nagagawa S, Laws R, Jamieson I (2011) Multimodel inference in ecology and evolution: challenges and solutions. J Evol Biol 24:699–711

Harms S, Winant C (1998) Characteristic patterns of the circulation in the Santa Barbara Channel. J Geophys Res 103:3041–3065

Hickey B (1979) The California Current System — hypotheses and facts. Prog Oceanogr 8:191–279

Hickey B (1992) Circulation over the Santa Monica-San Pedro basin and shelf. Prog Oceanogr 30:37–115

Hickey B (1993) Physical oceanography. In: Dailey M, Reish D, Anderson J (eds) Ecology of the Southern California Bight. University of California Press, Berkeley, CA, p 19–70

Hickey B, Dobbins E, Allen S (2003) Local and remote forcing of currents and temperature in the central Southern California Bight. J Geophys Res 108:3081

Hobson KA (1999) Tracing origins and migration of wildlife using stable isotopes: a review. Oecologia 120:314–326

Hobson K, Piatt J, Pitocchelli J (1994) Using stable isotopes to determine seabird trophic relationships. J Anim Ecol 63:786–798

Hobson K, Barnett-Johnson R, Cerling T (2010) Using isoscapes to track animal migration. In: West J, Bowen G, Dawsom T, Tu K (eds) Isoscapes: understanding movement, pattern, and process on Earth through isotope mapping. Springer, New York, NY, p 273–298

Jaeger A, Lecomte V, Weimerskirch H, Richard P, Cherel Y (2010) Seabird satellite tracking validates the use of latitudinal isoscapes to depict predators' foraging areas in the Southern Ocean. Rapid Commun Mass Spectrom 24: 3456–3460

Jennings S, Warr K (2003) Environmental correlates of large-scale spatial variation in the $\delta^{15}N$ of marine animals. Mar Biol 142:1131–1140

Kérouel R, Aminot A (1997) Fluorometric determination of ammonia in sea and estuarine waters by direct segmented flow analysis. Mar Chem 57:265–275

Kurle CM (2009) Interpreting temporal variation in omnivore foraging ecology via stable isotope modeling. Funct Ecol 23:733–744

Kurle CM, Gudmundson CJ (2007) Regional differences in foraging of young-of-the-year Steller sea lions *Eumetopias jubatus* in Alaska: stable carbon and nitrogen isotope ratios in blood. Mar Ecol Prog Ser 342:303–310

Kurle CM, Worthy GAJ (2001) Stable isotope assessment of temporal and geographic differences in feeding ecology of northern fur seals (*Callorhinus ursinus*) and their prey. Oecologia 126:254–265

Kurle CM, Worthy GAJ (2002) Stable nitrogen and carbon isotope ratios in multiple tissues of the northern fur seal *Callorhinus ursinus*: implications for dietary and migratory reconstructions. Mar Ecol Prog Ser 236:289–300

Kurle C, Sinclair E, Edwards A, Gudmundson C (2011) Temporal and spatial variation in the $\delta^{15}N$ and $\delta^{13}C$ values of common marine prey species from Alaskan waters. Mar Biol 158:2389–2404

Laakmann S, Auel H (2010) Longitudinal and vertical trends in stable isotope signatures ($\delta^{13}C$ and $\delta^{15}N$) of omnivorous and carnivorous copepods across the South Atlantic Ocean. Mar Biol 157:463–471

Landry MR, Lorenzen CJ, Peterson WK (1994) Mesoplankton grazing in the Southern California Bight. II. Grazing impact and particulate flux. Mar Ecol Prog Ser 115:73–85

Longhurst A (1995) Seasonal cycles of pelagic production and consumption. Prog Oceanogr 36:77–167

Lorrain A, Graham B, Popp B, Allain V and others (2014) Nitrogen isotopic baselines and implications for estimating foraging habitat and trophic position of yellowfin tuna in the Indian and Pacific Oceans. Deep Sea Res II 113:188–198

Lynn R, Simpson J (1987) The California Current System: the seasonal variability of its physical characteristics. J Geophys Res 92:12947–12966

MacKenzie K, Longmore C, Preece C, Lucas C, Trueman C (2014) Testing the long-term stability of marine isosapes in shelf seas using jellyfish tissues. Biogeochemistry 121: 441–454

Mantyla A, Bogard S, Venrick E (2008) Patterns and controls of chlorophyll-*a* and primary productivity cycles in the Southern California Bight. J Mar Syst 73:48–60

McMahon K, Hamady L, Thorrold S (2013) A review of ecogeochemistry approaches to estimating movements of marine animals. Limnol Oceanogr 58:697–714

Nakatsuka T, Handa N, Wada E, Wong C (1992) The dynamic changes of stable isotopic ratios of nitrogen and carbon in suspended and sedimented particulate organic matter during a phytoplankton bloom. J Mar Res 50: 267–296

Newsome S, Clementz M, Koch P (2010) Using stable isotope biogeochemistry to study marine mammal ecology. Mar Mamm Sci 26:509–572

Owen R (1980) Eddies of the California Current System: physical and ecological characteristics. In: Power D (ed) The California islands. Museum of Natural History, Santa Barbara, CA, p 237–263

Pethybridge H, Young J, Kuhnert P, Farley J (2015) Using stable isotopes of albacore tuna and predictive models to characterize bioregions and examine ecological change in the SW Pacific Ocean. Prog Oceanogr 134:293–303

Popp B, Laws E, Bidigare R, Dore J, Hanson K, Wakeham S (1998) Effect of phytoplankton cell geometry on carbon isotopic fractionation. Geochim Cosmochim Acta 62: 69–77

Popp B, Graham B, Olson R, Hannides C and others (2007) Insight into the trophic ecology of yellowfin tuna, *Thunnus albacares* from compound-specific nitrogen isotope analysis of proteinaceous amino acids. In: Dawson T, Siegwolf R (eds) Stable isotopes as indicators of ecological change. Elsevier, New York, NY, p 173–190

Quillfeldt P, Ekschmitt K, Brickle P, McGill R, Wolters V, Dehnhard N, Masello J (2015) Variability of higher torphic level stable isotope data in space and time — a case study in a marine ecosystem. Rapid Commun Mass Spectrom 29:667–674

Radabaugh K, Hollander D, Peebles E (2013) Seasonal $\delta^{13}C$ and $\delta^{15}N$ isoscapes of fish populations along a continental shelf trophic gradient. Cont Shelf Res 68:112–122

Ramos R, Gonzalez-Solis J (2012) Trace me if you can: the use of intrinsic biogeochemial markers in marine top predators. Front Ecol Environ 10:258–266

Ramos R, Gonzalez-Solis J, Croxall J, Oro D, Ruiz X (2009) Understanding oceanic migrations with intrinsic biogeochemical markers. PLOS ONE 4:e6236

Rau G, Sweeney R, Kaplan I (1982) Plankton ^{13}C:^{12}C ratio changes with latitude: differences between northern and southern oceans. Deep-Sea Res 29:1035–1039

Rau G, Takahashi T, Des Marais D (1989) Latitudinal variations in plankton $\delta^{13}C$: implications for CO_2 and productivity in past oceans. Nature 341:516–518

Rau GH, Teyssie JL, Rassoulzadegan F, Fowler SW (1990) $^{13}C/^{12}C$ and $^{15}N/^{14}N$ variations among size-fractionated marine particles: implications for their origin and trophic relationships. Mar Ecol Prog Ser 59:33–38

Rau GH, Takahashi T, Des Marais DJ, Repeta DJ, Martin JH (1992) The relationship between $\delta^{13}C$ of organic matter and $[CO_2(aq)]$ in ocean surface-water: data from a JGOFS site in the northeast Atlantic Ocean and a model. Geochim Cosmochim Acta 56:1413–1419

Rau G, Chavez F, Friederich G (2001) Plankton $^{13}C/^{12}C$ variations in Monterey Bay, California: evidence of non-diffusive inorganic carbon uptake by phytoplankton in an upwelling environment. Deep Sea Res I 48:79–94

Raven JA (1994) Carbon fixation and carbon availability in marine phytoplankton. Photosynth Res 39:259–273

Raven J, Johnston A, Turpin D (1993) Influence of changes in CO_2 concentration and temperature on marine phytoplankton $^{13}C/^{12}C$ ratios: an analysis of possible mechanisms. Global Planet Change 8:1–12

Rubenstein DR, Hobson KA (2004) From birds to butterflies: animal movement patterns and stable isotopes. Trends Ecol Evol 19:256–263

Ruiz-Cooley R, Gerrodette T (2012) Tracking large-scale latitudinal patterns of $\delta^{13}C$ and $\delta^{15}N$ along the eastern Pacific using epi-mesopelagic squid as indicators. Ecosphere 3:art63

Ruiz-Cooley R, Koch P, Fiedler P, McCarthy M (2014) Carbon and nitrogen isotopes from top predator amino acids reveal rapidly shifting ocean biochemistry in the outer California Current. PLOS ONE 9:e110355

Schell D (2000) Declining carrying capacity in the Bering Sea: isotopic evidence from whale baleen. Limnol Oceanogr 45:459–462

Schell DM, Barnett BA, Vinette KA (1998) Carbon and nitrogen isotope ratios in zooplankton of the Bering, Chukchi, and Beaufort Seas. Mar Ecol Prog Ser 162:11–23

Schimmelmann A, Albertino A, Sauer P, Qi H, Molinie R, Mesnard F (2009) Nicotine, acetanilide and urea multilevel ^{2}H-,^{13}C- and ^{15}N-abundance reference materials for continuous-flow isotope ratio mass spectrometry. Rapid Commun Mass Spectrom 23:3513–3521

Smith S, Henrichs S, Rho T (2002) Stable C and N isotopic composition of sinking particles and zooplankton over the southeastern Bering Sea shelf. Deep Sea Res II 49: 6031–6050

Somes C, Schmittner A, Galbraith E, Lehmann M and others (2010) Simulating the global distribution of nitrogen isotopes in the ocean. Global Biogeochem Cycles 24: GB4019

Takekawa J, Carter H, Orthmeyer D, Golightly R and others (2004) At-sea distribution and abundance of seabirds and marine mammals in the Southern California Bight: 1999–2003. US Geological Survey, Western Ecological Research Center and Humboldt State University, Vallejo, CA and Arcata, CA

Trueman C, MacKenzie K, Palmer M (2012) Identifying migrations in marine fishes through stable-isotope analysis. J Fish Biol 81:826–847

Turner Tomaszewicz CN, Seminoff JA, Peckham SH, Avens L, Kurle CM (2017) Intrapopulation variability in the timing of ontogenetic habitat shifts in sea turtles revealed using $\delta^{15}N$ values from bone growth rings. J Anim Ecol, doi:10.1111/1365-2656.12618

Venrick E, Hayward T (1984) Determining chlorophyll on the 1984 CalCOFI surveys. California Cooperative Oceanographic and Fisheries Investigations. Data Rep XXV:74–79

Vokhshoori NL, Larsen T, McCarthy MD (2014) Reconstructing $\delta^{13}C$ isoscapes of phytoplankton production in a coastal upwelling system with amino acid isotope values of littoral mussels. Mar Ecol Prog Ser 504:59–72

Wu J, Calvert S, Wong C (1999) Carbon and nitrogen isotope ratios in sedimenting particulate organic matter at an upwelling site off Vancouver Island. Estuar Coast Shelf Sci 48:193–203

Editorial responsibility: Yves Cherel, Villiers-en-Bois, France

Submitted: May 26, 2016; Accepted: January 3, 2017
Proofs received from author(s): March 7, 2017